Transient Angle Stability Analysis of Grid-Connected Converters with the First-order Active Power Loop

Heng Wu, Xiongfei Wang
Department of Energy Technology, Aalborg University, Aalborg, Denmark
hew@et.aau.dk, xwa@et.aau.dk

***Abstract*—As the increasing application of power electronic converters in electric power grids, the stability of grid-connected converters has become a major concern for reliable operations of the power grid. This paper analyzes the transient stability of grid-connected converters with the first-order active power loop. It points out that the conventional equal-area criterion, which has been widely used in the transient stability analysis of synchronous generators, may not apply to grid-connected converters, due to the different dynamic characteristics between converters and synchronous generators. To tackle this challenge, this paper employs the phase portrait to analyze the transient stability of power converters, and it is found that the better transient stability performance can be achieved if the grid-connected converters are controlled as the first-order nonlinear system. Simulations and experimental results are given to verify the effectiveness of the theoretical analysis.**

Keywords—transient stability, grid-connected converters, phase portrait, active power control

I. INTRODUCTION

The increasing use of power electronic converters in power systems has drawn more attention to the control and stability of converter-grid interactions. In general, the stability issues can be categorized into two types, i.e. the small-signal stability and the large-signal stability (transient stability) [1]. Over the past few years, many research efforts have been made to study the small-signal stability of grid-connected converters [2]-[6]. However, the transient stability issue, which is the ability of grid-connected converters to maintain synchronism under severe grid disturbances, has not drawn much attention. The major difficulty in this area lies in extracting the large-signal dynamic behavior of grid-connected converters, where the small-signal modeling method and the linear control theory do not apply.

The equal-area criterion (EAC) has been widely used to analyze the transient stability of the synchronous generator (SG)-based power system [1]. This method can also be adopted to analyze the transient stability of grid-connected converters which are controlled to mimic dynamics of SGs, e.g. virtual synchronous generator (VSG) control [7]-[10]. Yet, the grid-connected converter can also be controlled to behave differently from the SG, e.g. the first-order active power loop like power synchronization control [11] and vector current control [12]. It is questionable whether the conclusion of the EAC is still applicable with the first-order active power loop. To fill this gap, the phase portrait is used in this paper to analyze the transient stability of grid-connected converters. It is found out that the EAC may yield invalid stability predictions for grid-connected converters, and the better transient stability performance can be achieved for the grid-connected converters controlled as a first-order nonlinear system.

The rest of the paper is organized as follows. Section II reviews the basics of transient stability analysis for traditional SG-based power systems. Three commonly used active power control schemes for grid-connected converters, i.e. the power synchronization control, the vector current control and the VSG control are then introduced in Section III. Differing from the VSG control, the power synchronization control and vector current control belongs to first-order active power loop and have significant different transient behavior. Therefore, the impacts of these two control schemes on the transient stability of the grid-connected converters are analyzed by means of the phase portrait in Section IV. Simulations and experimental results are given in Section V to corroborate the effectiveness of the theoretical analysis. Section VI concludes this paper.

II. REVIEW OF THE TRANSIENT STABILITY ANALYSIS OF THE SG BASED POWER SYSTEM

This section gives a brief review of the transient stability analysis of the SG-based power systems. The system of Fig. 1 is considered, which consists of an SG delivering power to the infinite bus via two paralleled transmission lines. The swing equations of the SG can be expressed as follows [1]:

$$P_m - P_e = J\omega\frac{d\omega}{dt} \tag{1}$$

$$P_e = \frac{3V_tV_g}{X_s}\sin\delta \tag{2}$$

where P_m is the input mechanical power, P_e is the output electric power, J is the inertia of the SG. V_t and V_g are the root mean square (RMS) values of the SG terminal voltage and the infinite bus voltage, respectively. X_s is the equivalent impedance between SG and grid, and δ is the power angle. The P_e-δ relationship with both two transmission lines in

service is shown as the dashed line in Fig. 2. The transient disturbance is considered as one of the transmission line (e.g. X_{g1}) is suddenly cleared from the power system, which results in a larger X_s and the corresponding P_e-δ relationship is shown as the solid line in Fig. 2.

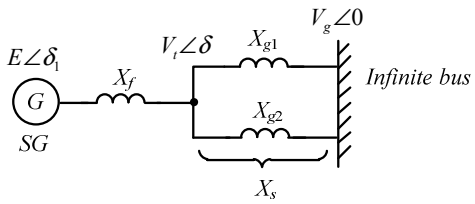

Fig. 1. An SG connecting to the infinite bus.

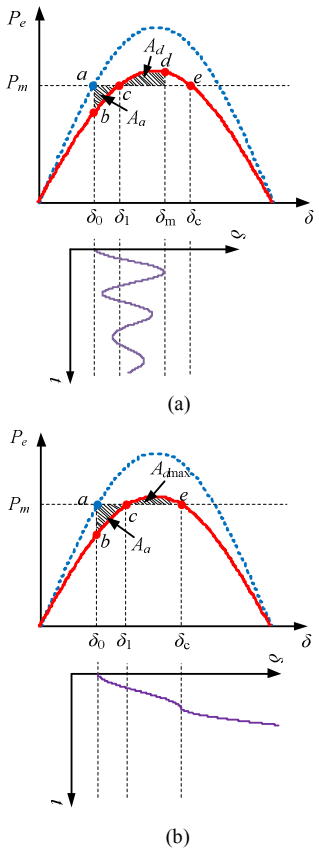

Fig. 2. P_e-δ curve before (dashed line) and after (solid line) the transient grid disturbance. (a) Stable case (b) Unstable case.

Based on (1), (2) and Fig. 2, the dynamic response of SG after the disturbance can be analyzed as follows: the operation point of the SG moves from *a* to *b* when the transient disturbance occurs, then the rotor of the SG starts to accelerate as $P_m>P_e$, which results in an increase in the power angle δ. The acceleration continues until it reaches the point *c*, where $P_m = P_e$. Yet, as the rotor speed is still above the synchronous speed ω_n at the point *c*, the power angle δ keeps increasing, while the rotor begins to decelerate after the point *c* due to the fact of $P_m<P_e$. Consequently, two possible operation scenarios are resulted:

1) The rotor speed recovers to its synchronous speed ω_n before the point *e*, e.g. the point *d* shown in Fig. 2(a). As $P_m<P_e$ still holds at the point *d*, the rotor further decelerates and results in a decrease in δ, and thus the operation point retraces the P_e-δ curve from *d* to *c* then to *b*. Such oscillations repeat several cycles and finally reaches to the steady state operation point *c* due to the damping effect [1]. The system finally becomes stable.
2) On the other hand, if the rotor speed is still above the synchronous speed even at the point *e*, as shown in Fig. 2(b), the rotor keeps accelerating after the point *e* as $P_m>P_e$ and the power angle δ keeps increase. As a result, the SG loses synchronism with the power grid and the system becomes unstable.

For the single machine infinite bus system, the transient stability performance of the SG is usually examined based on the EAC, which implies the SG system will be stable after transeint disturbance if it satisfies [1]

$$A_a \le A_{d\max} \tag{3}$$

where A_a is defined as the acceleration area, in which the rotor speed accelerates, and A_{dmax} is defined as the maximum deceleration area, in which the rotor decelerates, as shown in Fig. 2(b), and they can be calculated as

$$A_a = \int_{\delta_0}^{\delta_1} (P_m - P_e)\, d\delta \tag{4}$$

$$A_{d\max} = \int_{\delta_1}^{\delta_c} (P_e - P_m)\, d\delta \tag{5}$$

However, it should be noted that the EAC is derived based on the mathematical model of SGs [1], and it is not applicable for analyzing the transient stability of the grid-connected converter if it is controlled to behave differently from the SG. In fact, the grid-connected converter can become stable even if it does not satisfy the conclusion of the EAC, which will be shown in this work.

III. Active Power Control Schemes of Grid-Connected Converters

Fig. 3 shows the one-line diagram of a three-phase grid-connected converter, where a constant dc-link voltage (V_{dc}) is assumed. The grid-connected converter feeds power to the grid via two parallel transmission lines X_{g1} and X_{g2}, and X_g represents the equivalent grid impedance, where $X_g = X_{g1}//X_{g2}$. X_f represents the impedance of the output filter of the converter. The voltage and current at the point of common coupling (PCC) are measured to provide the information for the control system (including active/reactive control power loop, voltage/current control loop and the PLL). v_{PWMa}, v_{PWMb} and v_{PWMc} are the pulse width modulation (PWM) references generated from the control system employing different control algorithms.

Based on the discussion in Section II, the transient stability of grid-connected converters are mainly affected by the active power control loops. Thus three commonly used active power control schemes, i.e., 1) the power synchronization control, 2)

the VSG control, and 3) the vector current control are investigated in this work, as shown in Fig. 4

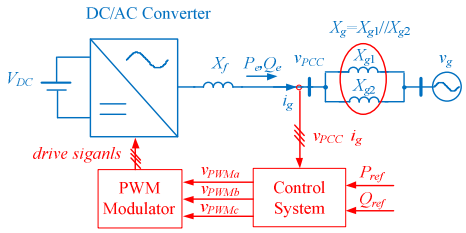

Fig. 3. One-line diagram of the grid-connected converter connecting to the weak ac network

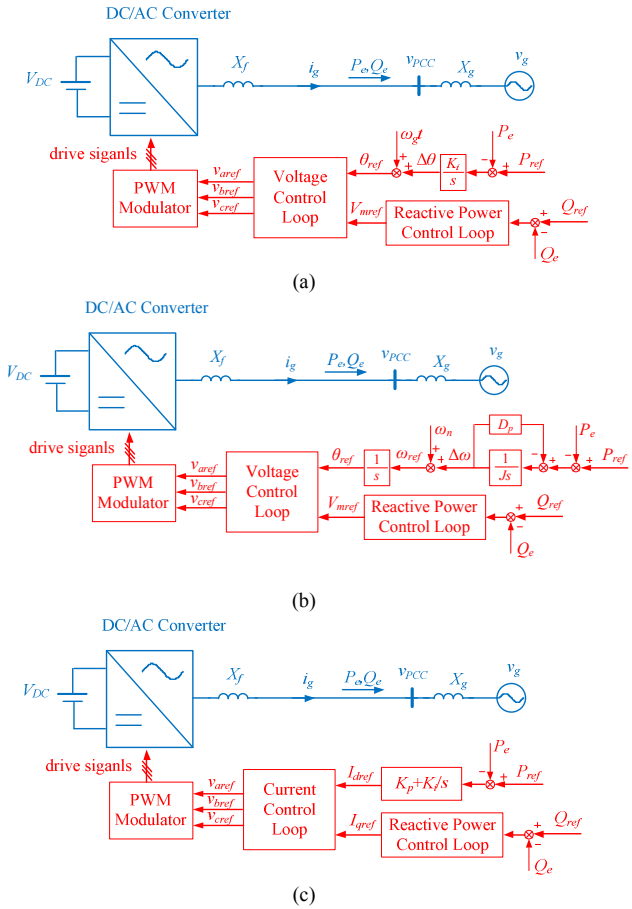

Fig. 4. One-line diagram of the grid-connected converter with different control schemes. (a) Power synchronization control. (b) VSG control (c) Active power loop for the current-mode control.

Since the timescale of the transient stability dynamic is generally within 2 s - 3 s after the initial disturbance [1], which is well decoupled from the timescales of inner voltage and current control loops (i.e. 1 ms - 10 ms) [13]. Therefore, only the dynamics of the active power loop is concerned, and the inner voltage and current loops can be regarded as a unity gain with the ideal reference tracking. Consequently, the block diagrams of these three active power control loops shown in Fig. 4 can be simplified, as illustrated in Fig. 5 [6], [11], [12], where δ is the power angle of the grid-connected converters, which is defined as the angle difference between the converter output voltage and grid voltage. It is noted that the active power loop for the power synchronization control and the vector current control can be approximated as a first-order nonlinear dynamic system, whereas the active power loop for the VSG control is equivalent to a second-order nonlinear dynamic systems.

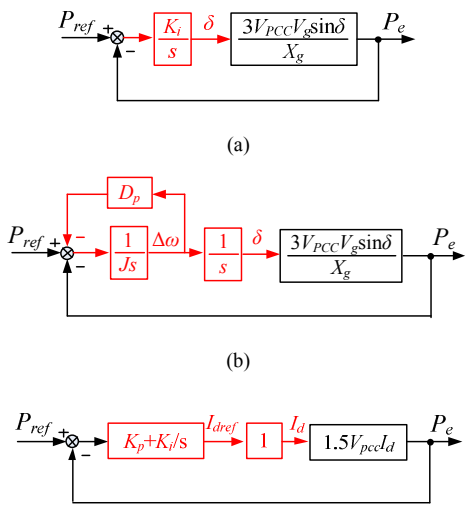

Fig. 5. Equivalent block diagram of active power control loop (a) Power synchronization control. (b) VSG control (c) Active power loop for the current-mode control.

IV. Transient Stability Analysis of Converter Based Power System

For grid-connected converters equipped with the VSG control, the EAC can still be used to access its transient stability behavior due to the similar power control dynamics between the VSG and the SG [7], [8]. However, the conclusion of EAC may no longer be valid for the transient stability analysis of the power synchronization control or the vector current control, since the first-order nonlinear system characteristic of these two control schemes are significantly different from that of SGs. New tools are thus demanded for the transient stability analysis of grid-connected converters with the first-order active power loop.

The phase portrait, which is a graphical tool widely used to analyze the first- and second-order nonlinear dynamic systems [14], is employed here for the transient stability analysis of the power synchronization control and the vector current control.

A. Phase Portrait Concept

The basic concept of the phase portrait is described below. Considering a general nonlinear differential equation given by

$$\dot{x} = f(x) \tag{6}$$

where x is the state variable of concern. Instead of solving $x(t)$ analytically, it is much easier to plot the $\dot{x} - x$ curve based on

(6), which is the so-called phase portrait [14], as shown in Fig. 6. Based on the phase portrait, the dynamic response of x can be analyzed as follows: x will increase (move rightwards in Fig. 6) if $\dot{x} > 0$, and will decrease (move leftwards in Fig. 6) if $\dot{x} < 0$, as the arrows indicated in Fig. 6. The points a and b represent the fixed points where $\dot{x} = 0$. The point a is a stable fixed point (also called sink) while the point b an unstable fixed point (also called source) [14]. This is because if the system initially operates at point a, it will return to this point after a small disturbance on x. In contrast, if the system initially operates at the point b, it will move away from this point after a small disturbance on x.

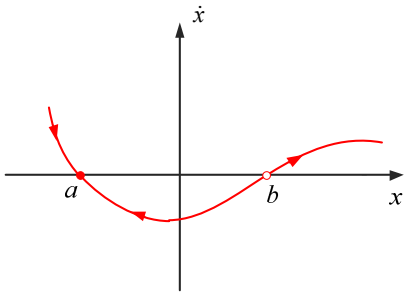

Fig. 6. An example of phase portrait

B. Power Synchronization Control

For power synchronization control, based on Fig. 5(a), we have

$$\begin{aligned}\dot{\delta} &= K_i\left(P_{ref} - \frac{3V_{PCC}V_g}{X_g}\sin\delta\right) \\ &\approx K_i\left(P_{ref} - \frac{3V_g^2}{X_g}\sin\delta\right)\end{aligned} \tag{7}$$

Based on (7), the phase portrait can be plotted, as shown in Fig. 7. The same disturbance described in Section II is considered here. The dashed line represents the phase portrait before the disturbance, while the solid line indicates the phase portrait after the disturbance, and the solid line with the arrow depicts the system trajectory. The system parameters are listed in Table I. From Fig. 7, the dynamic response of the converter after the disturbance can be analyzed as follows: the system operates at the point a ($\dot{\delta} = 0$) before the disturbance, and it suddenly moves to the point b at the instant when the disturbance occurs. Then, the power angle δ starts to increase (because $\dot{\delta} > 0$) until it reaches the point c ($\dot{\delta} = 0$), where the system comes into a new steady state at the point c. It is worth noting that such dynamic is significantly different from that of SGs, since the system keeps working at the point c after the first time it reaches to that point (due to $\dot{\delta} = 0$ at the point c), which implies that neither overshoot nor oscillation occurs in the transient period and it thus keeps the synchronism with the power grid. Thus, as a first-order nonlinear system, the power synchronization control shows a much better transient stability performance.

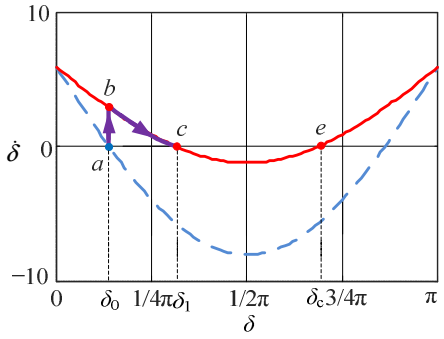

Fig. 7. Phase portrait of power synchronization control before (dashed line) and after (solid line) transient disturbance

Table I Parameters for transient disturbance test (case I)

Parameters			
P_{ref}	100 kW	L_f	0.5 mH
V_g	220 V	L_{g1}	3.8 mH
f_g	50 Hz	L_{g2}	4.9 mH

However, if the EAC is used to analyze the transient stability of the system, based on the parameters listed in Table I and (4)(5), it can be calculated that A_a=20233 W·rad, $A_{d\max}$=1230 W·rad. As $A_a >> A_{d\max}$, the conclusion of EAC indicates that the system should become unstable after transient disturbance, which is totally wrong, and it is further demonstrated that EAC is no longer valid to analyze the first-order nonlinear system.

C. Vector Current Control

Based on Fig. 5(c), the dynamic equations of the active power loop of the vector current control can be expressed as

$$I_d = \left(K_p + K_i\int\right)\left(P_{ref} - P_e\right) \tag{8}$$

Assuming that the converter is controlled for unity power factor operation, the relationship between the grid current, the PCC voltage and the grid voltage can be represented by the phasor diagram, as shown in Fig. 8

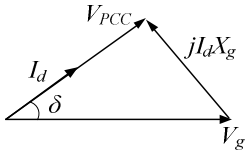

Fig. 8. Phasor diagram of current controlled converter with unity power factor.

Based on Fig. 8, the output active power can be expressed as

$$P_e = 3V_g I_d \cos\delta \tag{9}$$

The injected active current can be expressed as

$$I_d = \frac{V_g \sin\delta}{X_g} \tag{10}$$

Substituting (10) into (9) yields

$$P_e = \frac{3V_g^2}{X_g}\sin\delta\cos\delta = \frac{3V_g^2}{2X_g}\sin 2\delta \tag{11}$$

Substituting (10) and (11) into (8) yields

$$\frac{V_g \sin\delta}{X_g} = \left(K_p + K_i \int\right)\left(P_{ref} - \frac{3V_g^2}{2X_g}\sin 2\delta\right) \tag{12}$$

Applying the differentiator on the power angle δ at both sides of (12), and rearranging the equation yields

$$\dot{\delta} = \frac{K_i\left(P_{ref}X_g - 1.5V_g^2\sin 2\delta\right)}{\left(V_g\cos\delta + 3K_pV_g^2\cos 2\delta\right)} \tag{13}$$

Table II summarizes the main parameters used in this analysis. Based on (13), the phase portrait is plotted in Fig. 9, where the dashed line represents the phase portrait before the disturbance, while the solid line depicts the phase portrait after the disturbance, and the solid line with the arrow indicating the system operating trajectory.

Table II Parameters for transient disturbance test (case II)

Parameters			
P_{ref}	50 kW	L_f	0.5 mH
V_g	220 V	L_{g1}	3.8 mH
f_g	50 Hz	L_{g2}	4.9 mH

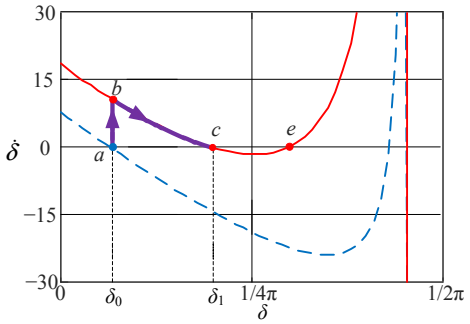

Fig. 9. Phase portrait of current-mode control before (dashed line) and after (solid line) transient disturbance

Since the active power loop of the vector current control is also equivalent to a first-order nonlinear system, the analysis procedure is similar to that of power synchronization control. As $\dot{\delta}=0$ also holds at the point c with the vector current control, the system keeps operating at the point c after the first time it reaches to that point and never crosses it, implying the overdamped transient response. Hence, the current-controlled converter with the first-order active power controller never has the transient stability problem.

However, based on the parameters listed in Table II and (4)(5), it can be calculated that A_a= 5030 W·rad, $A_{d\max}$= 362 W·rad, as $A_a >> A_{d\max}$, which indicates that the EAC lead to incorrect stability prediction for the first-order nonlinear system.

V. Simulation and Experimental Results

For verification, time-domain simulations and experiments are carried out considering the transient disturbance described in Section II. The parameters in Table I are adopted for the VSG control and the power synchronization control, while the parameters in Table II are adopted for the vector current control. With both sets of parameters, the acceleration area is much larger than the deceleration area (A_a=20233 W·rad, $A_{d\max}$=1230 W·rad, i.e. $A_a >> A_{d\max}$ for Table I, while A_a= 5030 W·rad, $A_{d\max}$=362 W·rad, $A_a >> A_{d\max}$ for Table II). Based on the EAC, the converter will lose synchronism with the power grid and become unstable after the disturbance.

Fig. 10(a) shows the simulation results for the VSG control. The oscillation in the converter output power, the power angle and three-phase grid currents can be observed in the simulated waveform. However, as discussed in Section IV, the converter will have no transient stability problem when the power synchronization control is adopted, which is verified in Fig. 10(b), where the overdamped response can be observed in the output power and the power angle. For same reason, similar overdamped dynamic responses can also be observed for the converter with the vector current control, as shown in Fig. 10(c). It can be seen that the system is also kept stable after the disturbance.

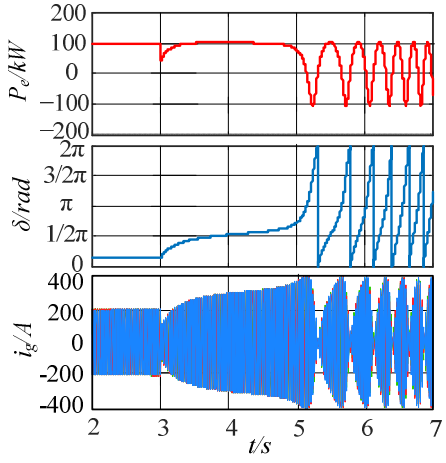

(a)

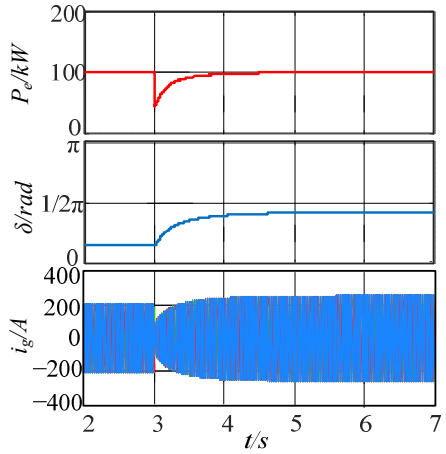

(b)

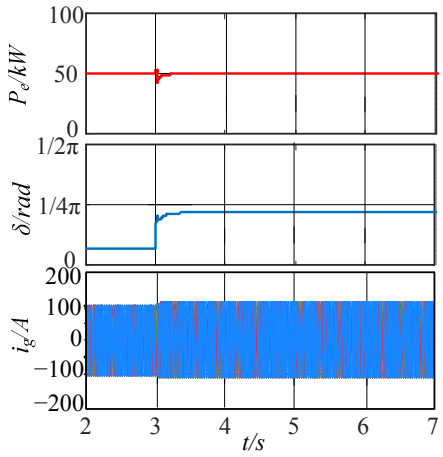

(c)

Fig. 10 Simulation results of dynamic response of converter under transient disturbance (a) VSG control (b) Power synchronization control (c) Current-mode control

Experimental tests are carried out based on the downscaled 1 kW grid-connected converter with a similar transient disturbance. The corresponding measurement results are given in Fig. 11. Similar to the simulation results, the unstable response can be observed for the converter with the VSG control, as shown in Fig. 11(a), while the stable operation can be observed for the converter with the power synchronization control and vector current control, as shown in Fig. 11(b) and (c). Obviously, both the simulations and experimental results agree well with the theoretical analysis.

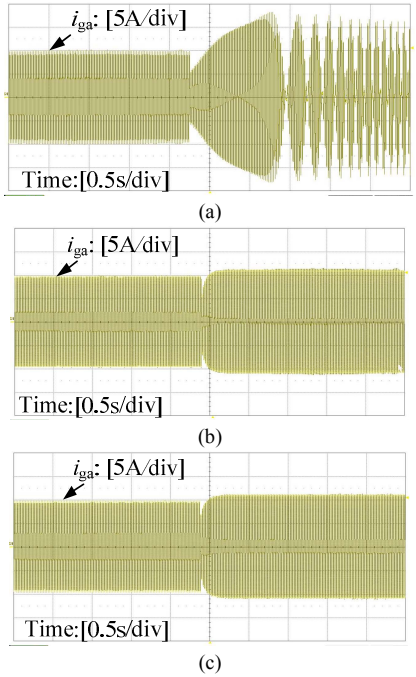

Fig. 11 Experimental results of dynamic response of converter under transient disturbance (a) VSG control (b) Power synchronization control (c) Current-mode control

VI. Conclusion

By using the phase portrait, this paper has provided the comprehensive study of transient stability issues of the grid-connected converters with the first-order active power loop. It has been revealed that the better transient stability performance of grid-connected converters than that of SGs can be achieved if their active power loop can be equivalent as a first-order nonlinear system. The simulation and experimental results have been given to verify the effectiveness of the theoretical analysis.

References

[1] P. Kundur. *Power System Stability and Control*. New York: McGraw-Hill, 1994.

[2] L. Harnefors, M. Bongiorno, and S. Lundberg, "Input-admittance calculation and shaping for controlled voltage-source converters," *IEEE Transactions on Industrial Electronics*., vol. 54, no. 6, pp. 3323-3334, Dec. 2007.

[3] X. Wang, F. Blaabjerg, and W. Wu, "Modeling and analysis of harmonic stability in an AC power-electronics-based power system," *IEEE Transactions on Power Electronics*., vol. 29, no. 12, pp. 6421-6432, Dec. 2014.

[4] X. Wang, L. Harnefors, and F. Blaabjerg, " Unified impedance model of grid-connected voltage-source converters," *IEEE Trans. Power Electron*., vol. 33, no. 2, pp. 1775-1787, Feb. 2018.

[5] D. Yang, X. Ruan, and H. Wu. "Impedance shaping of the grid-connected inverter with LCL filter to improve its adaptability to the weak grid condition," *IEEE Transactions on Power Electronics*., vol. 29, no. 11, pp. 5795-5805, Nov. 2014.

[6] H. Wu, X. Ruan, D. Yang, X. Chen, W. Zhao, Z. Lv, and Q. Zhong. "Small-signal modeling and parameters design for virtual synchronous generators". *IEEE Transactions on Industrial Electronics*, vol. 63 no, 7, pp. 4292−4303, July. 2016.

[7] L. Xiong, F. Zhuo, F. Wang, X. Liu, Y. Chen, M. Zhu, and H. Yi. "Static synchronous generator model: A new perspective to investigate dynamic characteristics and stability issues of grid-tied PWM inverter". *IEEE Transactions on Power Electronics*., vol. 31, no. 9, pp. 6264−6280, Sept. 2016.

[8] J. Alipoor, Y. Miura, and T. Ise. "Power system stabilization using virtual synchronous generator with alternating moment of inertia". *IEEE Journal of Emerging and Selected Topics in Power Electronics*, vol. 03, no. 2, pp. 451-458, June. 2015.

[9] H.-P. Beck and R. Hesse. "Virtual synchronous machine". in *Proc. 9th Int.Conf. EPQU*, 2007, pp. 1–6.

[10] Q. Zhong and G. Weiss. "Synchronverters: Inverters that mimic synchronous generators". *IEEE Transactions on Industrial Electronics*, vol. 58, no. 4, pp. 1259–1267, Apr., 2011.

[11] L. Zhang, L. Harnefors, and H. P. Nee. "Power-synchronization control of grid-connected voltage-source converters". *IEEE Transactions on Power Systems*., vol. 25, no. 2, pp. 809−820, May. 2010.

[12] R. Teodorescu, M. Liserre, and P. Rodriguez. *Grid-connected converters for photovoltaic and wind power systems*. Wiley-IEEE Press, 2011.

[13] Y. Hao, X. Yuan, and J. Hu "Modeling of grid-connected VSCs for power system small-signal stability analysis in DC-Link voltage control timescale" *IEEE Trans. Power Syst.,* early access.

[14] Steven H. Strogatz. *Nonlinear Dynamics and Chaos: With Applications to Physics, Biology, Chemistry, and Engineering*. Perseus Books, 1994